AIAA Aviation
August 12-14, 2013, Los Angeles, CA
2013 Aviation Technology, Integration, and Operations Conference

Real-Time Air Traffic Flow Estimation for Improved Situational Awareness in the Terminal Area

Bong-Jun Yang* and P.K. Menon†
Optimal Synthesis Inc., Los Altos, CA, 94022

The problem of estimating the characteristics of the air traffic flow in the Terminal Area is considered. The estimated parameters can be used by the Traffic Flow Coordinators and Terminal Area Controllers to improve their response to varying air traffic flow. The approach is based on a queuing abstraction of the arrival and departure traffic routes in the Terminal Area. The routes are discretized as spatial servers for enforcing FAA-mandated separation requirements. Particle filtering methodology is employed for estimating the time-varying queuing parameters using radar track data. By considering the waypoint crossing times and airspeed as measurements, it is shown that it is feasible to estimate the time delay and its rate at various points along the arrival-departure routes. The proposed approach is illustrated using arrival radar track data in the San Francisco Metroplex. A graphic display of estimated parameters to serve as decision support tool for use by the Terminal Area traffic controllers is also illustrated.

Downloaded by UNIVERSITY OF CALIFORNIA - BERKELEY on June 25, 2014 | http://arc.aiaa.org | DOI: 10.2514/6.2013-4236

I. Introduction

DECISION Support Tools (DSTs) for Traffic Flow Management (TFM) need the characterization of the current and future traffic situations for effective management. Several NASA efforts have investigated TFM using advanced iterative algorithms not only for strategic TFM in the National Airspace System (NAS) but also for managing surface traffic flows[1-8]. While these algorithms can provide precise solutions to the traffic management problem, they are more suitable for predictive control based on deterministic data. Traffic flow control in the presence of uncertainties inherent in the air traffic management system requires the integration of an estimation algorithm in the loop to derive the stochastic description of traffic flow, followed by the application of Statistical Decision Theory[9] to either trigger iterative numerical algorithms or to directly display the parameters to support real-time flow control decisions.

Queuing network models[10-13] capture the stochastic features of traffic flow using two sets of parameters, namely, the inter-arrival time distribution and service time distributions between every node in the network. Because the queuing model parameters are based on aggregated data, and because the queuing network can provide the statistical distributions of the variables of interest, the queuing network model is suitable for use as the basis for formulating stochastic estimation algorithms. A recent research effort [14-18] discusses a family of queuing network models suitable for modeling traffic flow in the NAS. It has been demonstrated[17] that these models can accurately predict the statistics traffic flow, at a fraction of the computational time required for explicit Monte-Carlo simulations.

In this paper, the flight operations in the terminal area are analyzed using a queuing network model. In deterministic approaches of trajectory-based operations, the route geometry in the terminal airspace is accurately modeled, and a high-fidelity flight dynamics model is utilized to propagate each flight along these routes[19,20]. These models generally require algorithms for trajectory prediction, and conflict detection-resolution. Tactical control mechanisms such as vectoring to maintain separation assurance have to be explicitly coded in the trajectory propagation equations. Stochastic analysis using such models is generally performed through Monte Carlo simulations. This process is computationally intensive, and may restrict their use to off-line computations.

On the other hand, gross queuing models that resort to the closed form solution of queuing equations do not model terminal route geometries and may use a single queue to represent the entire route from the arrival fix to the runway[21]. The flight arrival and service characteristics are aggregated into inter-arrival time distributions and service time distributions. The parameters of the queuing model are generally derived from historic data and may not be

* Research Scientist, 95 First Street, jun.yang@optisyn.com, Senior Member AIAA.
† Chief Scientist, 95 First Street, menon@optisyn.com, Fellow AIAA.

relevant with a different traffic volume or after the terminal route geometry is altered. This limits the use of such gross queuing models to concept analysis.

The queuing network models for charactering terminal area operations in the paper are presented in Reference 22, in which detailed terminal area route structures are considered while tactical control mechanisms are incorporated as queuing abstractions. The queuing models in Reference 22 consider high-fidelity route geometries of the terminal area, and separation among aircraft is ensured by enforcing the rule that only one aircraft can occupy a single server at a given time instant. The length of a server is determined such that separation constraint is always met. These queuing models were developed in order to support NASA Airspace Super-Density Operations research that aims to develop efficient terminal area operations. They provide high-fidelity characterizations of terminal area operations while maintaining computational efficiency.

The problem of estimating the parameters of high-fidelity queuing models of the Terminal Area routes is addressed in this paper. The updates on the parameter estimates are made using available measurements such as the position and speed of flights provided by the Terminal Area radars. As the route geometries are incorporated in detail in queuing models, the results in this paper are a natural extension of the estimation results in Reference 23 from the estimation scheme of a relatively simple queuing network to that of a complex queuing network. More precisely, while the route in Reference 23 consists of a single server, the route in this paper comprises multiple servers based on realistic arrival and departure routes in metroplexes. Additionally, whereas traffic density in regions of the airspace, flight time between waypoints and traffic flows at specific fixes are main traffic flow metrics in Reference 23, the time-delay and its rate are directly estimated by reformulated particle filters and treated as flow metrics. These features lead to information for decision making that is more meaningful to human controllers. The estimator formulation follows the *Bayesian* approach [24] of using measurements to update *prior* statistical distribution of queuing network parameters. Since the probability distributions employed in queuing networks are non-Gaussian, traditional estimation techniques such as Kalman Filters [25] cannot be used. However, rapid evolution of computer technology has made it possible to consider more advanced estimation schemes such as the particle filtering technique[26,27] for this non-Gaussian estimation problem.

The paper is organized as follows. In Section II, the high-fidelity queuing model is illustrated using the San Francisco metroplex area. In Section III, particle filtering implementation for estimating queuing parameters is presented. The particle filtering is performed at the level of each server, which can be parallelizable. Since the queuing parameters at the server level may be too detailed for use as a decision support aids to human controllers, aggregation of the information for use by the controllers is addressed in Section IV. A prototype of the display which provides real-time information on the time delay and its trend along various route segments is also discussed. Conclusions from the present research are in Section V.

II. Queuing Network Models of the Terminal Area Operations

The estimation approach for real-time decisions requires a baseline queuing model that can characterize the traffic flow in the terminal area. The estimation approach in this paper is illustrated using the San Francisco Terminal Area. The traffic flows in the San Francisco metroplex according to the West Plan are shown in Figure 1 (a). This metroplex includes San Francisco International Airport (KSFO), Oakland International Airport (KOAK), and Mineta San Jose International Airport (KSJC). The traffic flows into the area under the South East Plan is shown in Figure 1 (b). Figure 2 shows an example of arrival routes in the San Francisco metroplex. Based on the historical radar tracking data at SFO Metroplex, the common entry waypoints for KSFO are chosen as PYE, MOD, ANJEE, and PIRAT; the common entry waypoints for KOAK are STIKM, LOCKE and KARNN; and the common entry waypoints for KSJC are JEJMA and FEXUV. Ten arrival routes for the West Plan configuration are shown in Figure 2 because there are two routes that split at DUXBY from PYE to KSFO. These routes begin about 50 nautical miles from the center of the metroplex. The corresponding entry waypoints are highlighted in red in Figure 2. These routes are assembled using the Coded Instrument Flight Procedures (CIFP)[30] and historical radar track data. CIFP, formerly known as the National Flight Database (NFD), is a dataset modeled to the Airlines Electronic Engineering Committee (AEEC) Aeronautical Radio Incorporated (ARINC) Navigation System Data Base (NDB) international standard (ARINC 424). Data elements included in CIFP are: Airports and Heliports, VHF, NDB and ILS Navigation Aids, Fixes and Waypoints, Airways, Departure Procedures (DPs), Standard Terminal Arrival Routes (STARs), Special Use Airspace (SUAs) and Class B,C, and D Airspace. Also included are GPS, RNAV (GPS), RNAV (RNP), GPS Overlay and ILS Standard Instrument Approach Procedures (SIAPs) with their associated Minimum Safe Altitude (MSA) data. SIAPs and STARs provide guidelines to build these routes. Clustered routes from a set of historical radar track are also used as guidelines in building the network.

Downloaded by UNIVERSITY OF CALIFORNIA - BERKELEY on June 25, 2014 | http://arc.aiaa.org | DOI: 10.2514/6.2013-4236

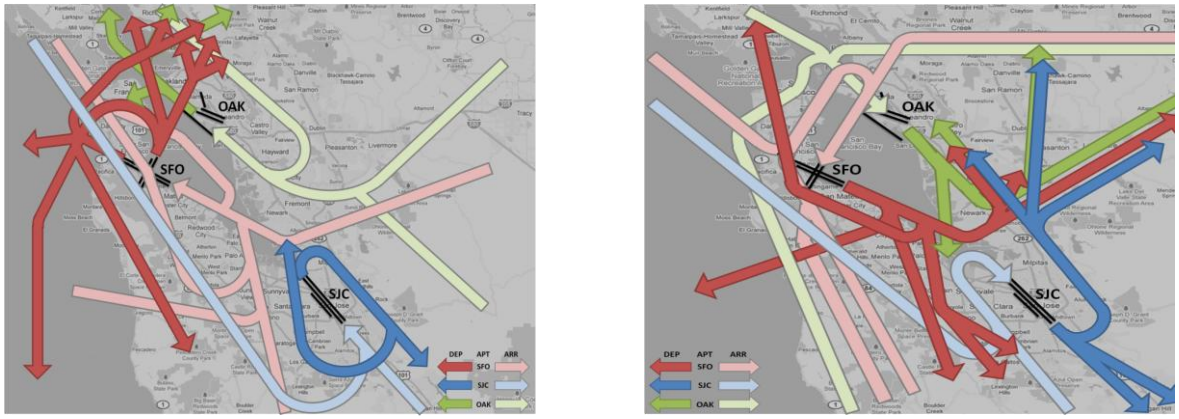

(a) West Plan **(b) South-East Plan**

Figure 1. San Francisco Bay Area Terminal Airspace Routes[29]

Figure 2. Arrival Routes at San Francisco Metroplex (West Plan)

Once the waypoints of the routes are assembled, the routes are converted into a set of servers as shown in Figure 3. In the present queuing network model, each server denotes a 3 nm segment along routes that can be occupied by only a single aircraft, thereby satisfying the required separation standards in the Terminal Area. The radar track data is next associated with the route layout. As an example, Figure 2 shows some of the West Plan tracks on October 1, 2010 into Runways 28L and 28R at KSFO, Runway 29 at KOAK and Runways 30R at KSJC. As can be observed from Figure 2 and Figure 3, the present queuing models inherently enforce the separation of flights and can model detailed variations in route structures. These variations can occur due to weather, traffic densities in certain areas, and runway configuration changes.

Downloaded by UNIVERSITY OF CALIFORNIA - BERKELEY on June 25, 2014 | http://arc.aiaa.org | DOI: 10.2514/6.2013-4236

Downloaded by UNIVERSITY OF CALIFORNIA - BERKELEY on June 25, 2014 | http://arc.aiaa.org | DOI: 10.2514/6.2013-4236

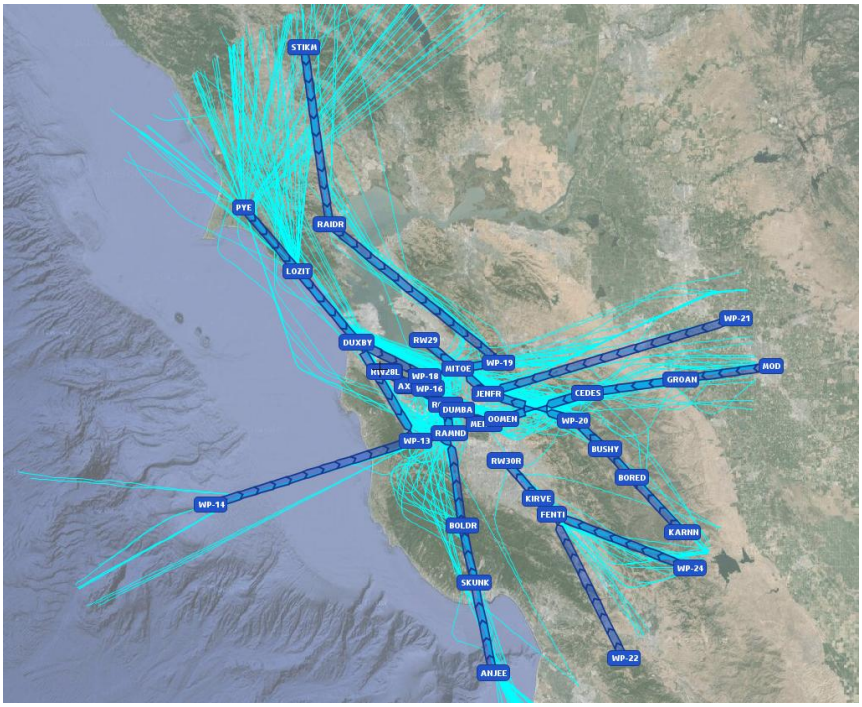

Figure 3. Queue Model of San Francisco Metroplex (West Plan)

III. Particle Filter at Each Server

Once queuing models for the terminal area are constructed, the statistical distribution of queuing network parameters for traffic flow can be determined from historic traffic data. However, for real-time assessment of traffic flows, an approach must be found to update the parameter distributions derived from historic data to detect any changes requiring controller attention. This can be carried out using the Bayesian estimation approach[24,25] based on the radar track data. The Bayes estimation approach updates *prior* statistical distributions using *evidence* in the form of measurements to get *posterior* or updated distributions. A well-known implementation of this approach is the Kalman Filter[25]. The Kalman Filter is a Bayes estimator for linear dynamic systems with Gaussian noise components and derives recursive relationships of posterior distributions from prior distributions and measurements. Due to its elegance and computational efficiency, the Kalman Filtering technique has found applications in extremely diverse set of problems.

Unfortunately, the Kalman Filter approach cannot be employed in estimating the parameters of the queuing network because of two reasons. Firstly, the inter-arrival time distributions and service time distributions are all constrained to be greater than zero. Secondly, these distributions are not Gaussian and are typically described by Poisson, Erlang or Coxian distributions[10, 11]. These facts require the consideration of more advanced techniques such as particle filtering algorithms[24,26,27]. Particle filters belong to the class of filters known as nonparametric filters. They do not rely on a fixed functional form of the posterior distributions such as Gaussians. Instead, they approximate posteriors by a finite number of state samples (cloud of particles), each roughly corresponding to a region in the state space. As the number of particles goes to infinity, the particle distribution tends to converge uniformly to the correct posterior under certain smoothness assumptions. Particle filters do not make strong parametric assumptions on the posterior density and are well suited for representing complex, multimodal probability density functions. However, the representational power of these techniques comes at the cost of added computational complexity. The following subsection will briefly review general Bayes filtering approach.

A. Bayes Filter

Consider the following discrete time dynamic system:

$$x_{k+1} = f(x_k, v_k)$$
$$y_k = g(x_k, w_k) \quad (1)$$

where x_k is the state of the model at the k^{th} instant, y_k is the measurement, f denotes the time-propagation function, v_k is the process noise, and w_k is the measurement uncertainty in the measurement model function g. It is assumed

that their probability distributions are known. Let the accumulation of measurements up to the current time step k be denoted by Y_k, i.e., $Y_k := \{y_i \,|i = 1,2, \dots, k\}$. Then, the objective of filtering is to derive $p(x_k|Y_k)$, the probability density function of the state x_k conditioned on the accumulated measurements up to the k^{th} time step. Three following major steps constitute the Bayes filter.

1) The initial probability distribution $p(x_0) = p(x_0|Y_0)$ is assumed to be known.
2) Given the known initial distribution for the state, subsequent probability distributions are obtained recursively. Given a previous probability distribution $p(x_{k-1}|Y_{k-1})$, the posterior distribution $p(x_k|Y_k)$ is obtained by the following step.
    a. Prediction

$$p(x_k|Y_{k-1}) = \int_{x_{k-1}} p(x_k|x_{k-1})p(x_{k-1}|Y_{k-1})dx_{k-1}, \tag{2}$$

where $p(x_k|x_{k-1})$ is the transitional probability density that is governed by the time marching function $x_{k+1} = f(x_k, v_k)$ in Eq. (1).

    b. Update

$$p(x_k|Y_k) = \frac{p(z_k|x_k)p(x_k|Y_{k-1})}{p(y_k|Y_{k-1})}, \tag{3}$$

where $p(z_k|x_k)$ denotes the probability distribution of the output y_k conditioned on x_k and is governed by the measurement function $y_k = g(x_k, w_k)$ in Eq. (1).

As stated earlier, Kalman filter is special case of Bayes filter for linear system dynamics with white Gaussian noise components. Particle filter is a numerical implementation of the Bayes filter for nonlinear systems with non-Gaussian noises and uses the idea of Monte Caro simulation using a large number of samples for the state variable (particles).

B. Particle Filter Algorithm

Particle filter is an approximate realization of Bayes filter via the approximation of a probability density function by a set of samples for the state and associated probability (particles), i.e., $p(x_k|Y_k) \approx \sum_{i=1}^{N} w_k^i \delta(x_k - x^i)$, where N is the total number of particles. The first step in the particle filter algorithm is to initialize a set of particles according to the a priori distribution of the state at the first time step.

$$\{\ \hat{x}_0^i\ \}_{i=1}^N, \tag{4}$$

where $\hat{x}_0^i$ denotes the state of the i^{th} particle at the first time step. Then the following loop is recursively executed from the initial time to the final time step.

Begin Loop from Initial Time to Final Time

Once the measurement y_k is available at the current time, the weight ω_k^i for the i^{th} particle can be calculated as

$$\{\ \omega_k^i = p\left(y_k \middle| \hat{x}_k^i\right)\omega^i{}_{k-1}\ \}_{i=1}^N \tag{5}$$

Here, the particle weight denotes the probability that the particle generates the observed measurement. The particle weights are then normalized by dividing the weight of each particle by the sum of the weight of all particles as shown in Equations (6) and (7).

$$W = \sum_{i=1}^{N} \omega_k^i \tag{6}$$

$$\{\ \omega_k^i := \frac{\omega_k^i}{W}\ \}_{i=1}^N \tag{7}$$

Once the normalized particle weights are available, the forward state estimate is calculated as the weighted sum of the particles. Note that this provides the expected value of the state.

$$\hat{x}_k = \sum_{i=1}^{N} \omega_k^i \hat{x}_k^i \tag{8}$$

This is followed by the resampling step which draws N replacement particles from the current set of N particles, such that the probability of drawing each particle depends on its importance weight. The resampling step is a crucial part of the particle filtering algorithm. In the absence of resampling, many of the particles end up in regions of low posterior probability, which is called the degeneracy problem[27]. The resampling step generates a set of particles to the

Downloaded by UNIVERSITY OF CALIFORNIA - BERKELEY on June 25, 2014 | http://arc.aiaa.org | DOI: 10.2514/6.2013-4236

regions in the state space with high posterior probability and avoids the degeneracy problem. By doing so, the particle filter focuses the computational resources of the filter algorithm to the regions in the state space where they matter the most. Thus the performance of the filter is kept high with a smaller number of particles. Resampling need not be performed at every time step. It can be performed when the number of particles in regions of high posterior probability falls below a predefined threshold. The metric used to determine the number of particles in regions of high posterior probability is denoted by N_{eff} and is calculated as follows.

$$N_{eff} = \frac{1}{\sum_{i=1}^{N}(\omega_k^i)^2} \tag{9}$$

Typically, resampling is performed when the effective number of particles falls below $2/3$ of the total number of particles.

$$if\ N_{eff} < \frac{2}{3}N \qquad \{\ draw\ \hat{x}_k^i\ with\ probability\ \propto \omega_k^i\ \}_{i=1}^{N} \tag{10}$$

The resampling process generates particles with replacement. Note that the resampled particles are denoted by an under bar.

$$\left[\left\{\underline{\hat{x}_k^j}, \underline{\omega_k^j}\right\}_{j=1}^{N}\right] = RESAMPLE\ \left[\left\{\hat{x}_k^i, \omega_k^i\right\}_{i=1}^{N}\right] \tag{11}$$

There exist a few resampling methods in the literature[28]. For example, in multinomial resampling, the cumulative distribution function of the particle weights is calculated as shown by Equations (12) and (13).

$$c_1 = 0 \tag{12}$$

$$for\ \ i = 2{:}N \quad \{\ c_i = c_{i-1} + \omega_k^i\ \} \tag{13}$$

Then a uniform random number is generated between 0 and 1.

$$\{\ u_j \sim \mathbb{U}[0,1]\ \}_{j=1}^{N} \tag{14}$$

The index of the particle to be included in the resampled set is obtained from the following equation

$$\{\ find\ i, such\ that\ c_i \le u_j < c_{i+1}\ \}_{j=1}^{N} \tag{15}$$

The state of the i^{th} particle in the prior particle set is assigned to the j^{th} particle in the resampled set,and the importance weight is set uniformly.

$$\{\ \underline{\hat{x}_k^j} = \hat{x}_k^i\ ,\qquad \underline{\omega_k^j} = \frac{1}{\mathrm{N}}\ \}_{j=1}^{N} \tag{16}$$

Then the particles are propagated to the next time instant as shown by Equations (17) and (18). Since the individual particles are propagated numerically, any complex nonlinear function can be used in this particle filter framework. Eq. (18) shows how the sampling in Eq.(17) is performed; the process noise is sampled from a given noise distribution for the particle x_k^i, then the state at the next time step x_{k+1}^i is obtained by propagating the state with the sampled process noise following the system dynamics. Note that the noise process need not be additive as in Kalman filters. This is because the function f can be any form or any algorithm that can compute the next state given the state and the process noise.

$$\{\ sample\ \ \hat{x}_{k+1}^i \sim p(x_{k+1}|\hat{x}_k^i)\ \}_{i=1}^{N} \tag{17}$$

$$\{\ \hat{x}_{k+1}^i = f({x^i}_k, {v^i}_k)\ \}_{i=1}^{N} \tag{18}$$

This sequence of steps is continued till the final time step.

End Loop from Initial Time to Final Time

C. Queuing Network Parameter Estimation

Typical queuing analysis computes traffic flow metrics such as traffic intensity and waiting time (time delay) given the inter-arrival time distribution and the service time distribution. In the present research, recognizing that the service time distribution can be time-varying depending on traffic conditions, the service time and the ensuing flow metrics are estimated using available measurements in real-time. In particular, the time-delay is directly estimated at the server level. One immediate issue is that the estimation of the time-delay requires that the measured system time be divided between the service time and the time-delay. However, the single measurement of the system time is not

Downloaded by UNIVERSITY OF CALIFORNIA - BERKELEY on June 25, 2014 | http://arc.aiaa.org | DOI: 10.2514/6.2013-4236

sufficient to allow the estimation of time-delay. This issue is resolved by the fact that radar track data also provides the airspeed at waypoint crossings, and that the service time can be assumed as the unimpeded time for an aircraft to fly in the absence of additional flights. That is, the service time can be computed as the time that it takes for the aircraft to fly a direct path between the entry and exit for each server. The service time for each server can be computed as:

$$dt = \int_0^L \frac{ds}{V(s)}, \tag{19}$$

where s is the length of the server, $V(s)$ is the airspeed parameterized along the length of the path, and L is the length of the direct path from the entry node to the exit node. Moreover, if it is assumed that the airspeed varies linearly along the path, i.e., $V(s) = a\,s + b$, the integral can be evaluated as:

$$t_{svc} = \frac{1}{a}\ln\left(\frac{a}{b}L + 1\right), \tag{20}$$

where a is the slope of the airspeed variation along the path, b is the entry airspeed into the server. Note that the slope a can be computed from the available airspeeds.

Since both the time delay and its trend are important for initiating traffic flow management decisions, a continuous time-evolution model in time-delay estimation for each server is posed as follows.

$$\begin{aligned} \ddot{t_d} &= 0 \\ \dot{a} &= 0, \end{aligned} \tag{21}$$

where t_d is the time delay, and a is the slope of the rate of change of airspeed along the route segment. The measurements include the system time obtained from the waypoint crossing times, and entry and exit airspeeds. Since the state of the estimation model includes the slope of the airspeed variation along the straight path, the measurement for the slope for each server is computed as

$$y_2 = \frac{V_{exit} - V_{entry}}{L} + w_a(t), \tag{22}$$

where V_{exit} is the exit speed of the server, V_{entry} is the entry speed of the server, and $w_a(t)$ is the measurement noise caused by the noise in the airspeed measurement. With these assumptions, the discrete model for the time-delay estimation can be formulated as follows.

Time-Delay Evolution Model

$$\begin{aligned} a(t_2) &= a(t_1) + w_{ap}(t_1)\Delta T \\ x_1(t_2) &= x_1(t_1) + x_2(t_1)\Delta T + \frac{1}{2}\Delta T^2\, w_{tp}(t_1) \\ x_2(t_2) &= x_2(t_1) + \Delta T\, w_{tp}(t_1) \end{aligned} \tag{23}$$

In these equations, $(x_1, x_2) = (t_d, \dot{t}_d)$, $w_{ap}(\cdot)$ is the process noise for the slope of the airspeed variation, $w_{tp}(\cdot)$ is the process noise for the time-delay rate, and $\Delta T = t_2 - t_1$.

Measurement Model

By computing the slope for the airspeed variation along the path, the measurements available for estimation are as follows.

$$\begin{aligned} y_1(t_{2)} &= x_1(t_2) + t_{svc}(t_2) + w_s(t_2) \\ y_2(t_2) &= a(t_2) + w_a(t) \end{aligned} \tag{24}$$

where $w_s(\cdot), w_a(\cdot)$ are sensor noises, and $t_{svc}(t_2)$ is the service time given by

$$t_{svc}(t_2) = \begin{cases} \dfrac{1}{a(t_2)}\ln\left(\dfrac{a(t_2)}{V_{entry}}L + 1\right), & if\ a(t_2) \neq 0 \\ \dfrac{L}{V_{entry}}, & otherwise. \end{cases} \tag{25}$$

Figure 4 shows the particle filtering computations for each server.

Downloaded by UNIVERSITY OF CALIFORNIA - BERKELEY on June 25, 2014 | http://arc.aiaa.org | DOI: 10.2514/6.2013-4236

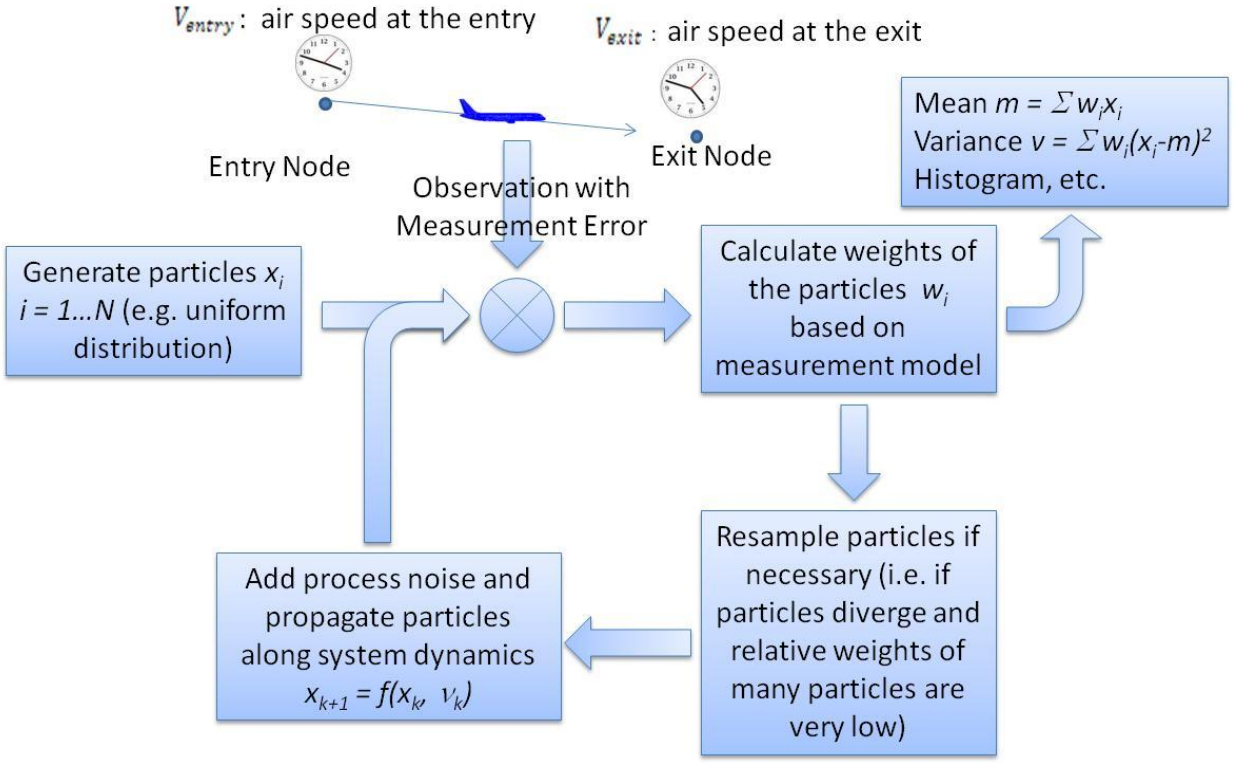

Figure 4. Particle Filtering Implementation for Each Server

D. A Real Traffic Example

Consider the flight VRD200 as shown in Figure 5. This flight occurred on 10/01/2010 in the SFO terminal area. VRD200 followed the route from ANJEE to KSFO and landed at Runway 28R. Figure 5(b) zooms in a portion of the route segment connected by the waypoint ANJEE to the merge waypoint ROKME and depicts how the server models are generated in the queuing network. In particular, the parameter distributions for severs 9-11 are monitored. The flight VRD200 is followed by SKW6832 and UAL73 depicted in Figure 6.

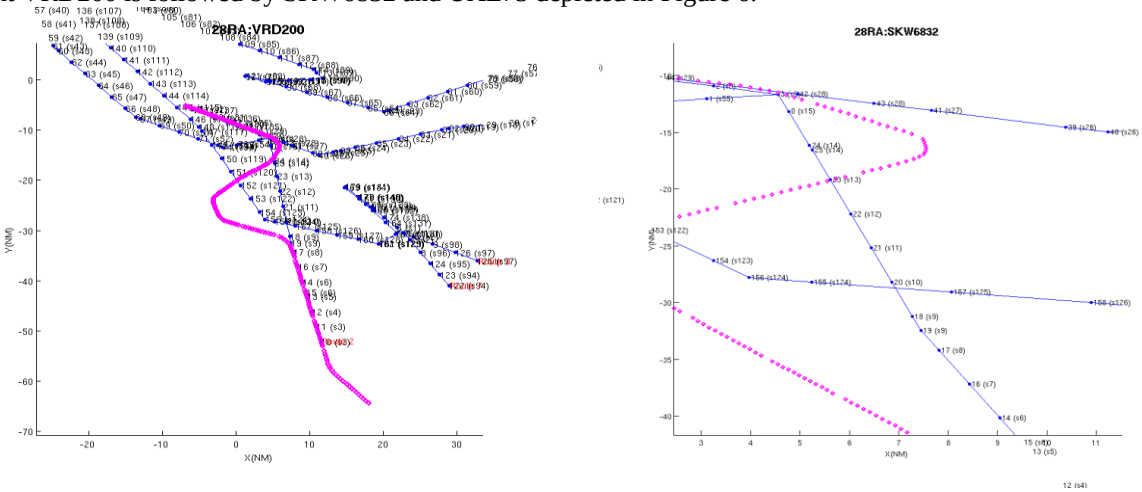

(a) Horizontal Trajectory **(b) Route Segment of Interest**

Figure 5. Flight VRD200

Downloaded by UNIVERSITY OF CALIFORNIA - BERKELEY on June 25, 2014 | http://arc.aiaa.org | DOI: 10.2514/6.2013-4236

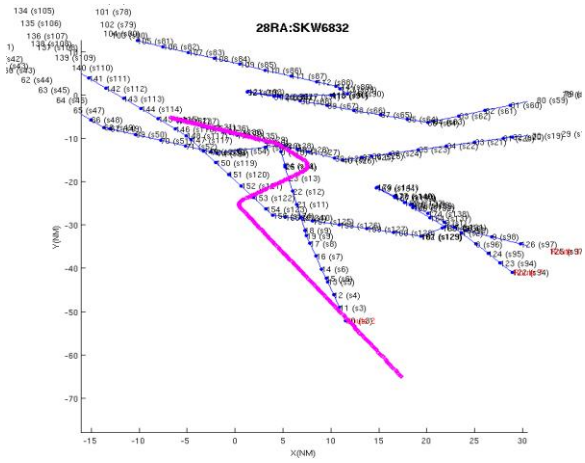

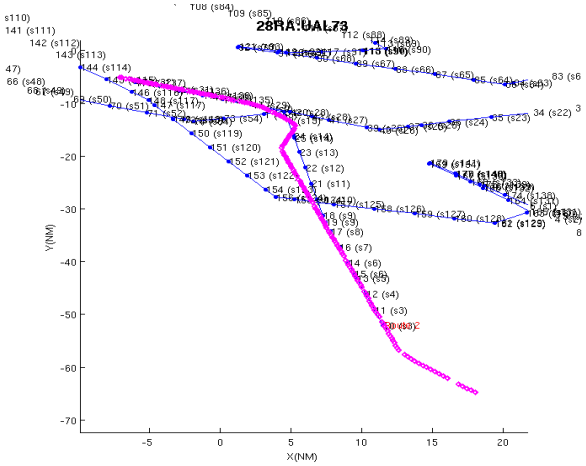

(c) SKW6832 Horizontal Trajectory **(d) UAL73 Horizontal Trajectory**

Figure 6. Horizontal Trajectories for UAL73 and SWA989

Figure 7 through Figure 9 shows the histograms for the time-delay and the service time. It can be observed that when the system time exhibits a significant increase due to the slower time of transit of flight SKW6832 (probably due to path stretching), the time delay distribution becomes wider, with a mean of -11.1553 seconds and a standard deviation of 33.7274 s, as shown in Figure 8 (a). Compared with the delay distribution, the service time distribution is much narrower because the airspeed measurement noise and the airspeed slope variation within 3 nm are small when compared with the time-delay variation caused by path stretching.

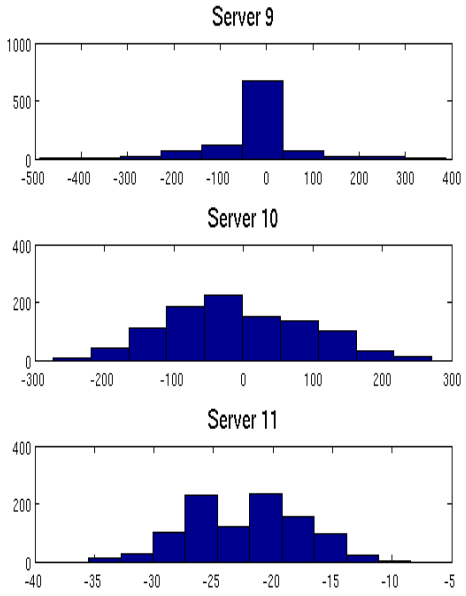

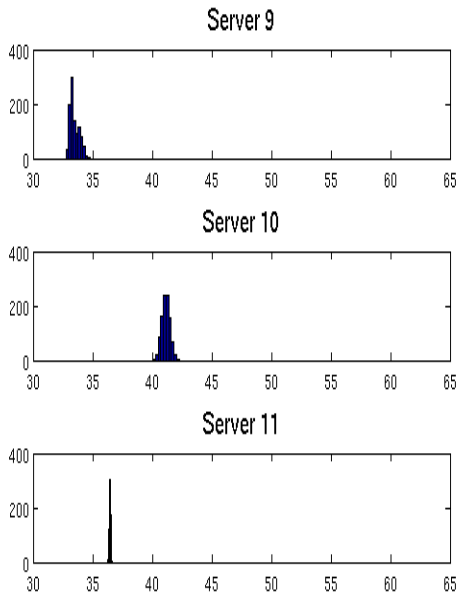

(a) Time Delay Histogram **(b) Service Time Histogram**

Figure 7. Histograms as Flight VRD200 Exits Server 11

Downloaded by UNIVERSITY OF CALIFORNIA - BERKELEY on June 25, 2014 | http://arc.aiaa.org | DOI: 10.2514/6.2013-4236

Downloaded by UNIVERSITY OF CALIFORNIA - BERKELEY on June 25, 2014 | http://arc.aiaa.org | DOI: 10.2514/6.2013-4236

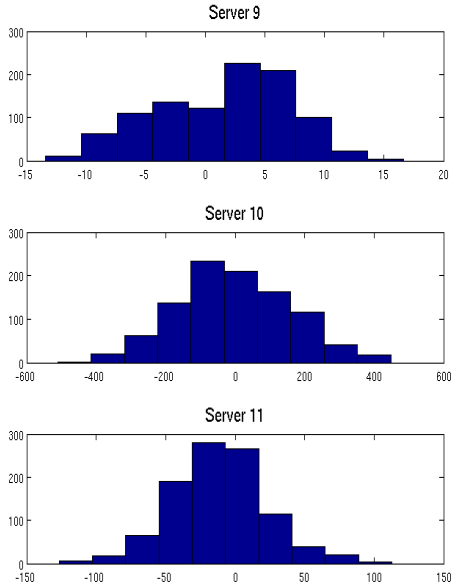

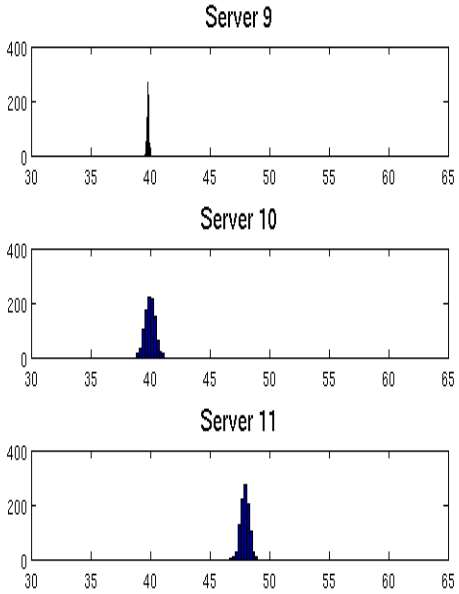

(a) Time Delay Histogram **(b) Service Time Histogram**

Figure 8. Histograms as Flight SKW6832 Exits Server 11

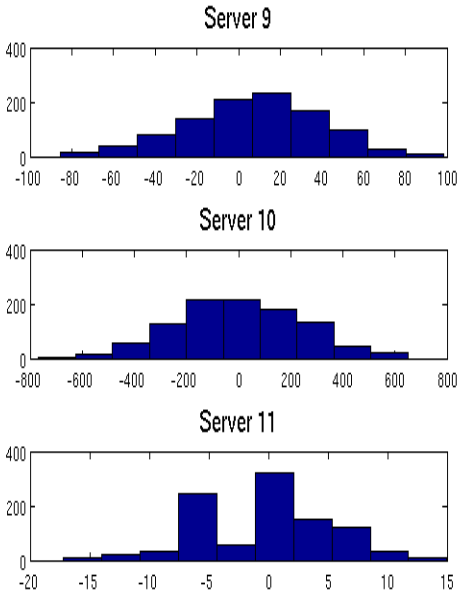

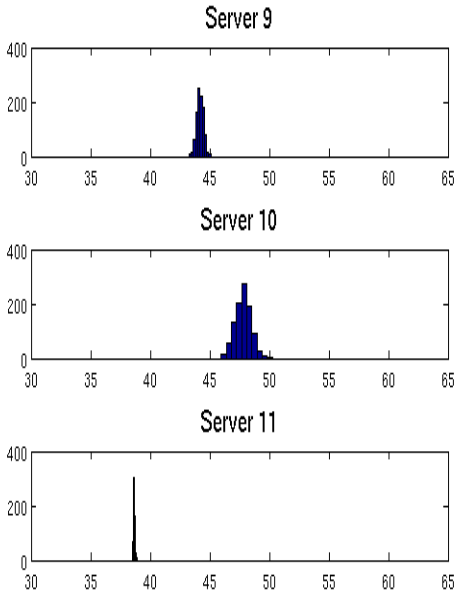

(a) Time Delay Histogram **(b) Service Time Histogram**

Figure 9. Histograms as Flight UAL73 Exits Server 11

IV. Traffic Information Display

While the implementation of particle filters for all the servers is highly parallelized and allows for a conceptually simple implementation, from the perspective of human monitoring of terminal area traffic, the delay information at the 3 nm server level is too detailed to be of use as decision support tool. Consequently, the flight times and delays in individual servers must be combined along the arrival route segments and displayed as histograms to the controllers. The following section discusses the methodology for carrying out the convolution computations.

A. Histogram Convolution

The particle filtering algorithm reports the probability distributions for variables of interest as histograms. Let a random variable be x, and its associated particles from the particle filtering be (x^j, w^j), $j = 1, \dots, N_p$. The probability distribution function for the random variable is approximated as $p(x) \approx \sum_{j=1}^{N_p} w^j \delta(x - x^j)$, where $\delta(\cdot)$ is the Kronecker-Delta function. Then, the histogram description for the probability density function, approximated by a set of particles, is obtained as follows. Let $x_0 < x_1 < \cdots < x_{N_h-1} < x_{N_h}$, with $x_i = i \cdot \Delta x$, be N_h intervals over which the histogram of the state values is constructed. Then, the bin height p_i, which is proportional to the probability of occurrence of the state in the ith interval, is calculated by the following relationship:

$$p_i \Delta x = P_r(x_{i-1} \le x < x_i) = \sum_{j \in A} w^j, \qquad A = \{j \,|\, x_{i-1} \le x^j < x_i\}. \tag{26}$$

Thus, particles that belong to each bin are collected and the sum of their weights constitutes the probability of the random variable belonging to each bin.

In order to compute the probability distribution of the time delay along a route segment, the histograms that represent the time delay probability density function at each server on the route segment are assembled by convolution. Let H_1 and H_2 bet two histograms represented by the following set of tuples:

$$H_1 = \{(x_0, p_0), (x_1, p_1), \dots, (x_{N_1-1}, p_{N_1-1})\}$$
$$H_2 = \{(y_0, q_0), (y_1, q_1), \dots, (y_{N_2-1}, q_{N_2-1})\} \tag{27}$$

A typical convolution algorithm for H_1 and H_2 leads to $N_1 + N_2 - 1$ number of bins for the resulting convolved histogram. Note that the number of bins increases as the number of convolutions increases. In the queuing network, a route segment can consist of several severs, and this increase in the bin number is not desirable.

The particle representation for a probability density function in the filter suggests a simple remedy for resolving the problem of increase in the number of bins. Accordingly, the convolution is implemented as follows. First, two histograms in Eq. (27) are viewed as a collection of particles. Thus, the probability distribution for the histograms are viewed as:

$$p(x) = \sum_{i=0}^{N_1-1} p_i \Delta x \, \delta(x - x_i)$$
$$p(y) = \sum_{j=0}^{N_2-1} q_j \Delta y \, \delta(y - y_j). \tag{28}$$

Secondly, since the random variable $z = x + y$ can take any value of $x_i + y_j$, $0 \le i \le N_1 - 1, 0 \le j \le N_2 - 1$, and the probability density function of the random variable can be approximated as:

$$p(z) = \sum_{i=0}^{N_1-1} \sum_{j=0}^{N_2-1} p_i \Delta x \, q_j \Delta y \, \delta(z - (x_i + y_j)) \tag{29}$$

In other words, the particle description for the convolved distribution is obtained by considering all the sample values possible by the particle description for the histogram in Eq. (28). The description in Eq. (29) is essentially the description of particles given by $(w_{ij}, z_{ij}) = (p_i q_j \Delta x \Delta y, x_i + y_j)$. Therefore, these particles are again collected into a

Downloaded by UNIVERSITY OF CALIFORNIA - BERKELEY on June 25, 2014 | http://arc.aiaa.org | DOI: 10.2514/6.2013-4236

histogram as done in Eq. (26). Note that the above convolution allows for the resulting convolved histogram to be displayed using any number of bins less than or equal to $N_1 + N_2 - 1$. Therefore, the convolved histogram can have a fixed number of bins specified by the user. Note that the fixed number of bins for the convolution histogram is achieved by adjusting the width of the bins. Repeating the above convolution algorithm successively leads to the convolved histogram for a route segment with its number of bins specified by the user.

B. A Departure Traffic Example at the LAX Metroplex

The convolution algorithms for time delay monitoring is illustrated using the queuing network depicted in Figure 10.

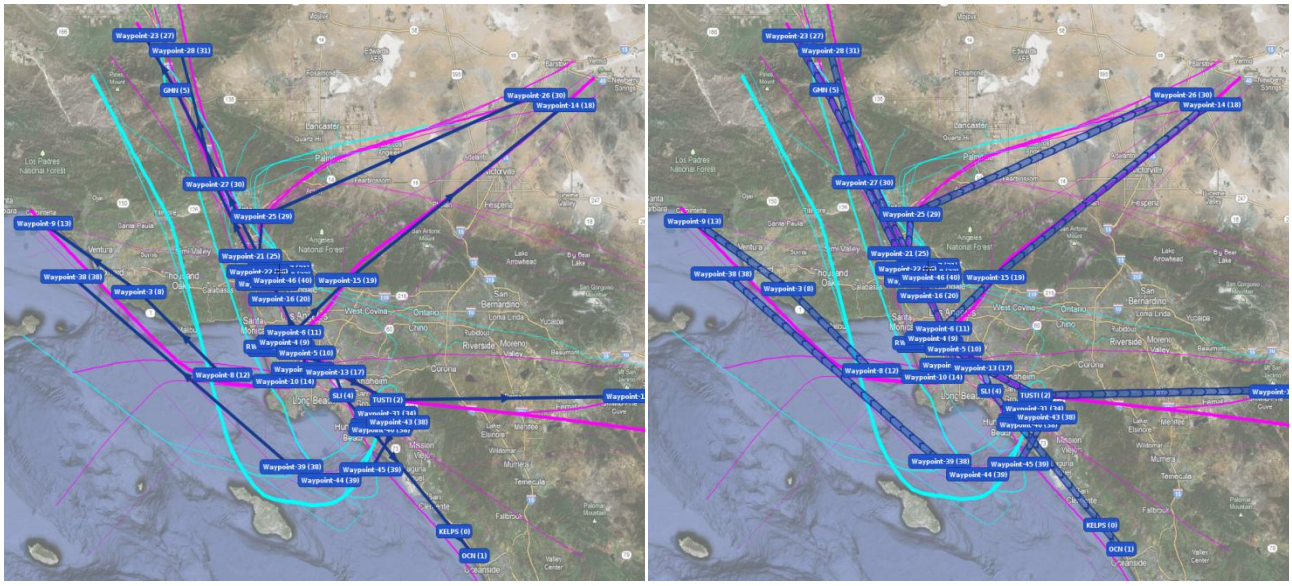

(a) Routes using Waypoint Representation **(b) Serverized Routes**

Figure 10. Departure Queuing Network for LAX Metroplex under the East Plan

The radar track of DAL2092 is displayed in comparison with departure routes in Figure 11. The flight DAL2092 took off from the runway 07L and was associated with Route 2. Each route consists of branches, which are used for displaying time delay information to human controllers as shown in Figure 12. Branches are in turn composed of servers, which are the fundamental elements in the queuing network for parameter estimation process described in Section III. Figure 13 shows that the branch 0 consists of three servers. In other words, time-delay and its rate, together with the service time, are estimated for each server by considering crossing times between the entry and exit nodes. Estimated time delay distributions for servers can be convolved to derive the time delay distribution for branches. The time delay distributions for branches can then be displayed on a graphical user interface for use by air traffic controllers.

Downloaded by UNIVERSITY OF CALIFORNIA - BERKELEY on June 25, 2014 | http://arc.aiaa.org | DOI: 10.2514/6.2013-4236

Downloaded by UNIVERSITY OF CALIFORNIA - BERKELEY on June 25, 2014 | http://arc.aiaa.org | DOI: 10.2514/6.2013-4236

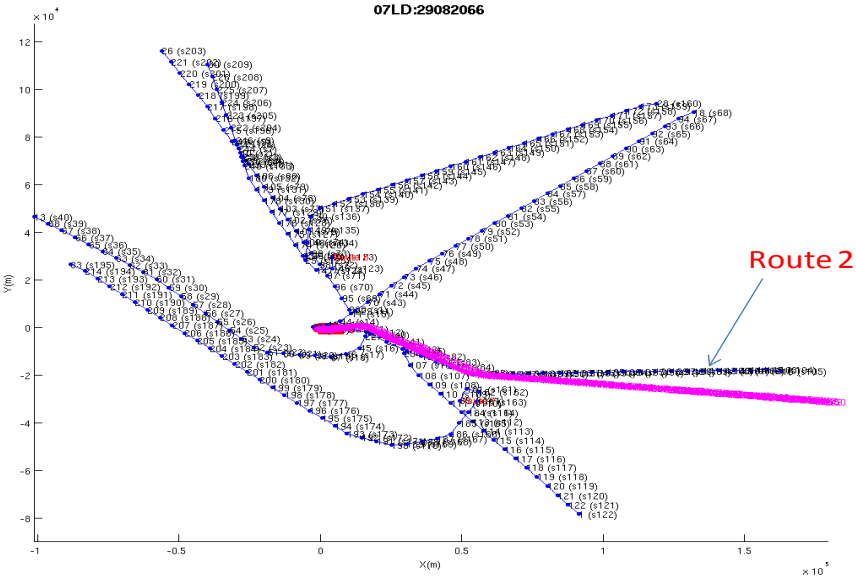

Figure 11. Track and Route Association

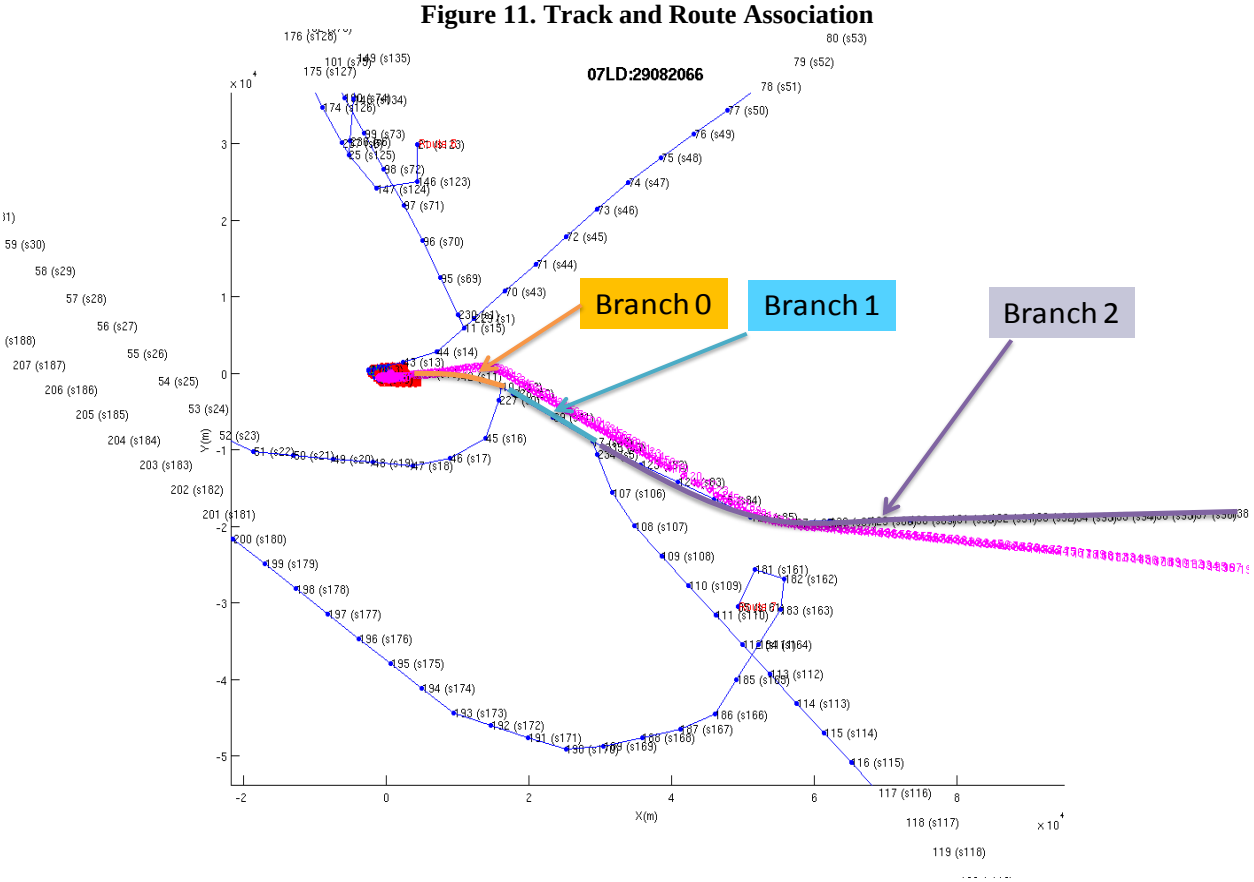

Figure 12. Decomposition of Route 2 by Branches

Downloaded by UNIVERSITY OF CALIFORNIA - BERKELEY on June 25, 2014 | http://arc.aiaa.org | DOI: 10.2514/6.2013-4236

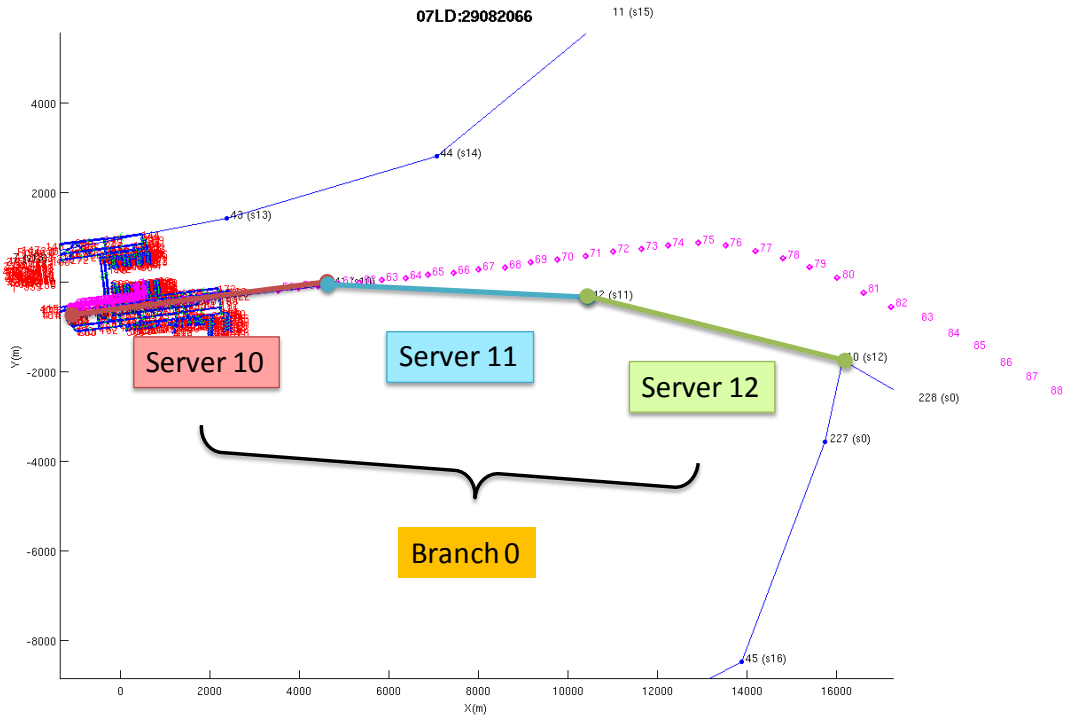

Figure 13. Decomposition of Branch by Servers

Figure 14 shows three consecutive flights that passed through Branch 0 consisting of servers 10, 11, 12. Time delay distributions in Server 12 after the passage of each flight are given in Figure 15. The time delay distribution for Branch 0 derived by the convolution of time delay distributions in individual servers is shown in Figure 16.

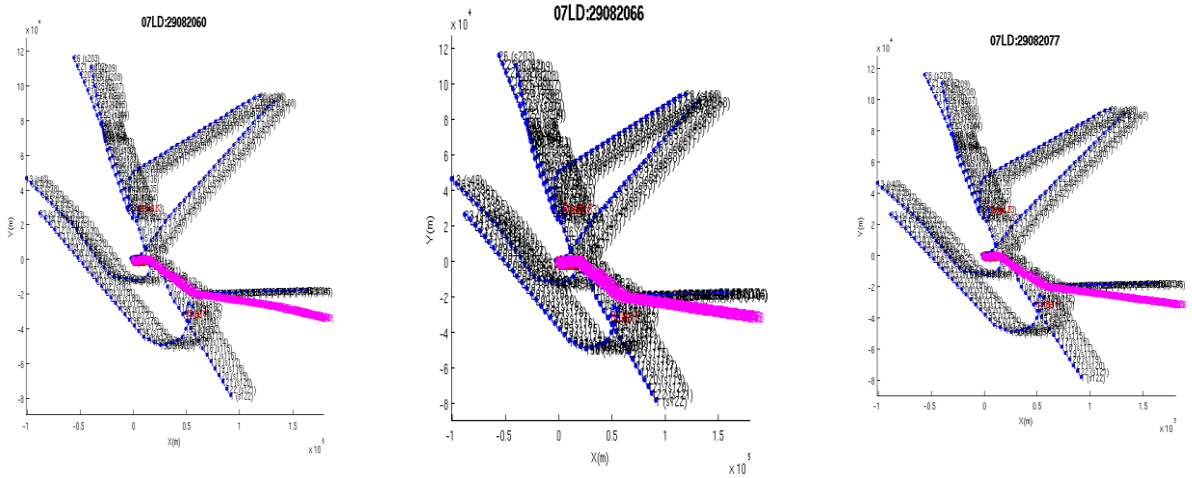

(a) AAL252 **(b) DAL2092** **(c) AAL144**

Figure 14. Example Radar Tracks

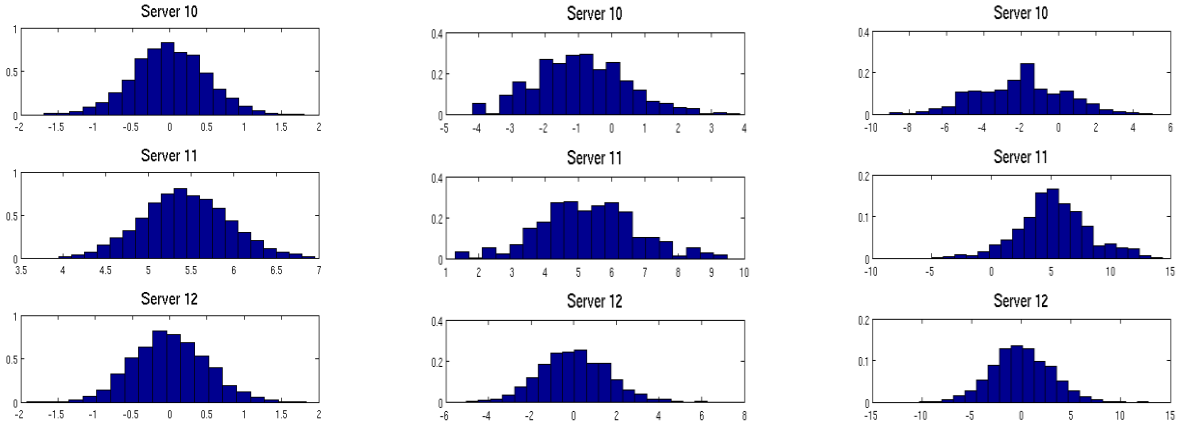

(a) When AAL252 leaves Server 12

(b) When DAL2092 Leaves Server 12

(c) When AAL144 Leaves Server 12

Figure 15. Evolution of Time Delay Distributions for Servers

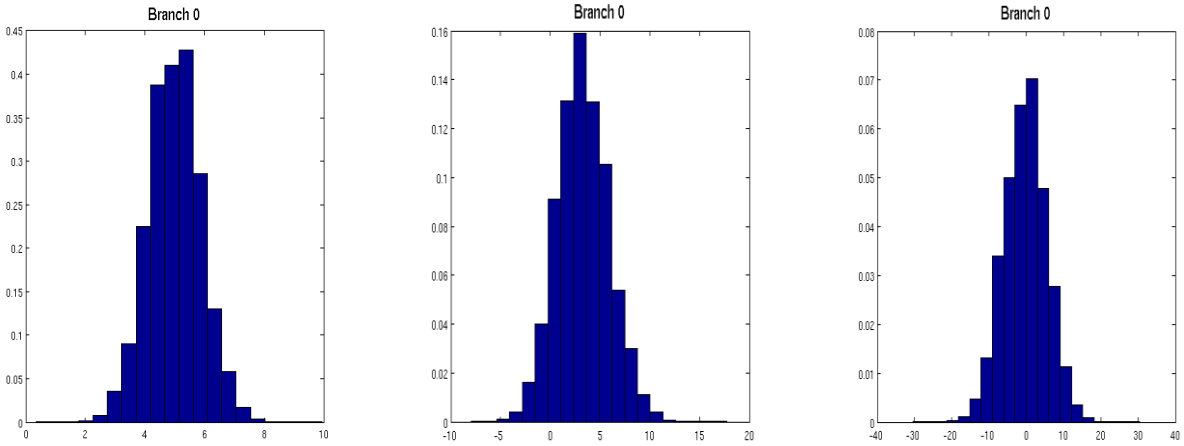

(a) When AAL252 leaves Server 12

(b) When DAL2092 Leaves Server 12

(c) When AAL144 Leaves Server 12

Figure 16. Time Delay Distributions for Branch 0

C. The Implementation of the Real-Time Traffic Estimator

Figure 17 shows the flowchart for the real-time traffic estimation using a historic radar track data. The estimation module reads the queuing network structure that is constructed using a queuing-network generation tool and configures the real-time estimator for the queuing network. The radar track file is read, and an instantaneous radar track snapshot is provided to the real-time estimator as measurements. Given the radar track measurements, the real-time estimator updates the estimates for the associated parameters of the queuing network and generates outputs for display for human controllers. The flowchart in Figure 17 is drawn under the assumption that the whole radar track in a file is processed, but this estimation process can be terminated at any time by the user of the real-time estimator.

Figure 18 elaborates the "Estimate Queuing-Network Parameters" block in Figure 17 and shows how an individual radar track is processed. The process updates the queuing network parameters once the aircraft has landed or departed. Each server updates the estimates of the service time, the time delay and the time delay rate for the arrival and departure networks. The server-level time delay information is then assembled via convolution for individual branches along the routes for display to the controllers. Each server performs particle filtering in order to estimate the queuing network parameters. The initialization for the particle filter is carried out when the server processes the first measurement.

Downloaded by UNIVERSITY OF CALIFORNIA - BERKELEY on June 25, 2014 | http://arc.aiaa.org | DOI: 10.2514/6.2013-4236

Downloaded by UNIVERSITY OF CALIFORNIA - BERKELEY on June 25, 2014 | http://arc.aiaa.org | DOI: 10.2514/6.2013-4236

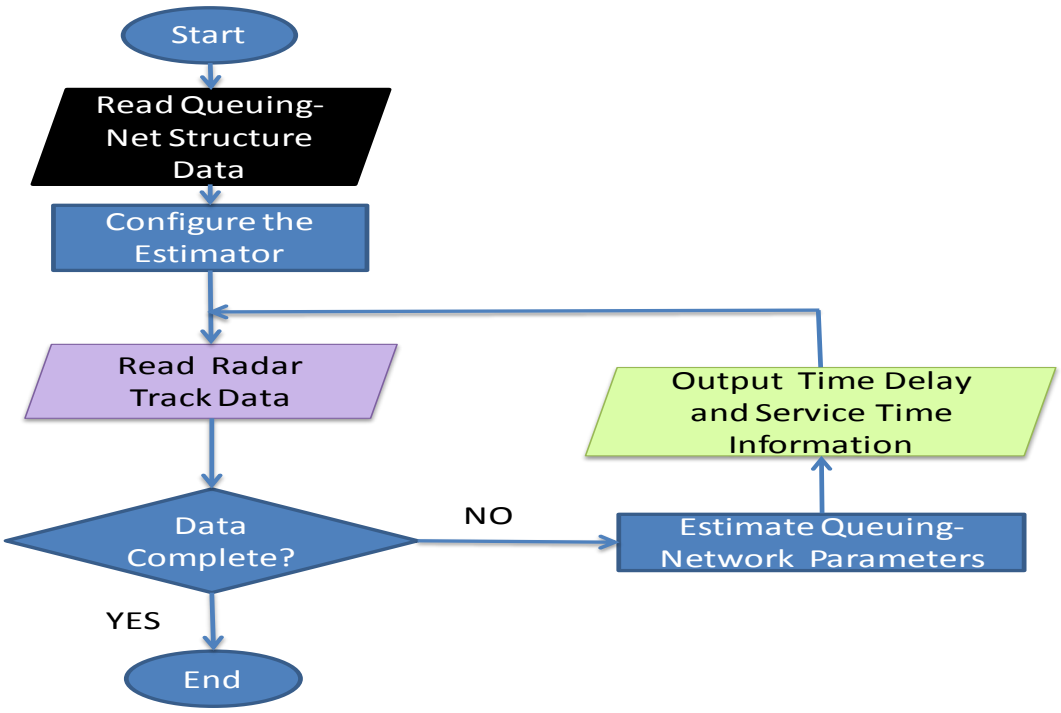

Figure 17. Flowchart of Flow Traffic Estimation

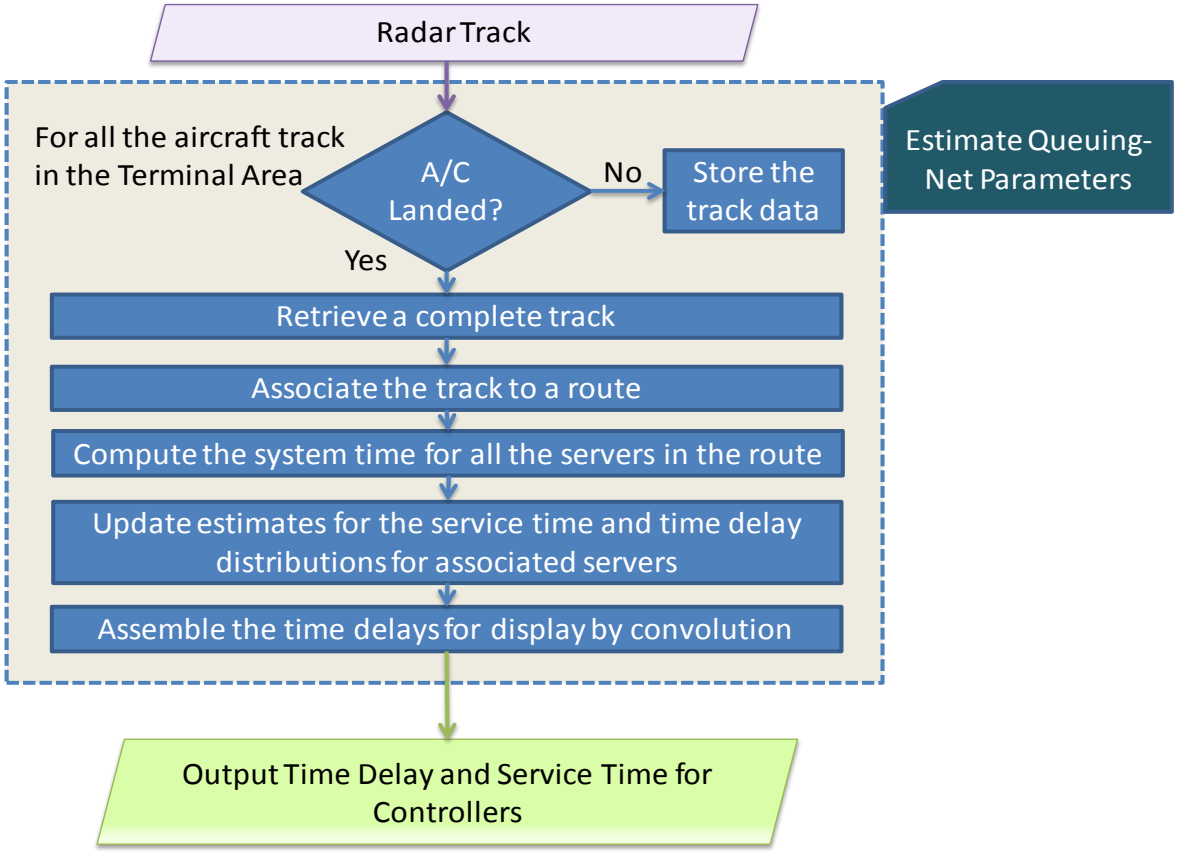

Figure 18. Details of the Parameter Estimation Function

D. Graphical User Interface for Displaying Traffic Flow Data to the Controller

The probability distribution for the delay and the time rate of the delay for each branch in the queuing network is updated whenever an aircraft passes the end node of the last server in the branch. In this section, a conceptual Graphical User Interface (GUI) for displaying the histograms is discussed. Figure 19 illustrates the display of histograms of the service time and the time delay for the branches of the arrival route from PYE to KSFO Runway 28R in the KSFO metroplex under the West Plan. Delay and flight time data for any other route can be displayed in a similar fashion.

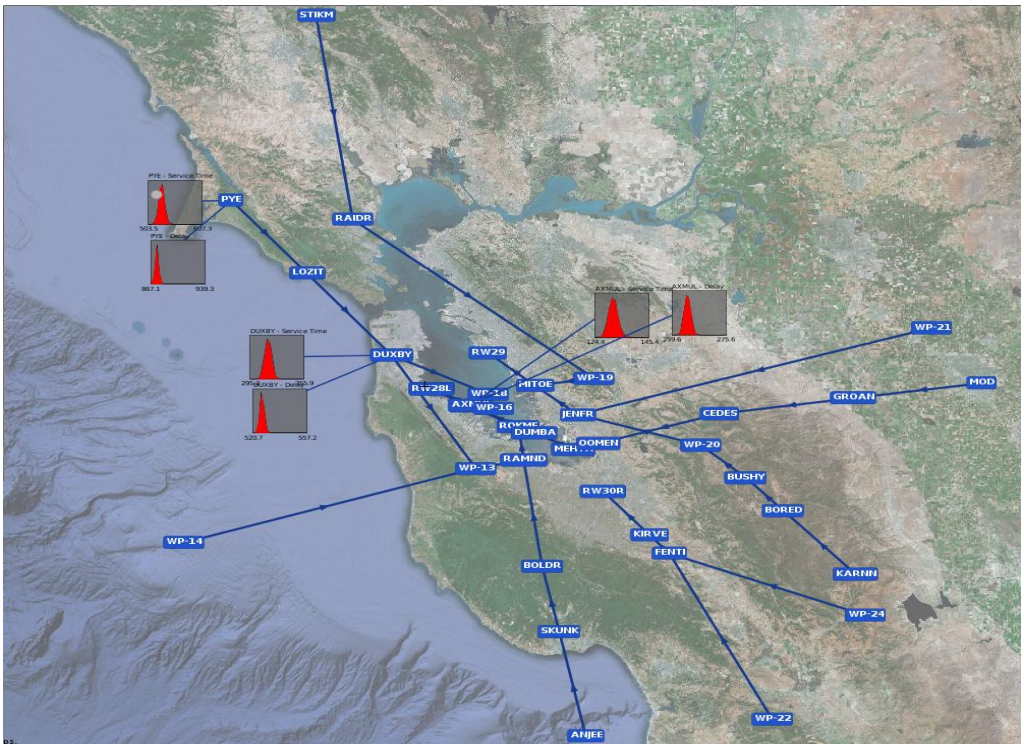

Figure 19. Histogram Displays for the Service Time and the Time Delay along Arrival Routes

The service time distribution along each route is the convolution of the service time distributions of every server along the route. As formulated in the present research, the service time depends entirely upon the route geometry and observed speeds of aircraft. As different types of aircraft exhibit different speed profiles in the terminal area, the service time variation is mostly due to the variations in the aircraft types. On the other hand, time delays are due to changes in the aircraft trajectories and are affected by path stretching and speed advisories issued by the air traffic controllers.

While the histogram displays in Figure 19 are useful for visually evaluating histograms of delays and service times in the queuing network by the analyst, it may not be useful as a real-time decision-support system. Figure 20 shows a more intuitive display for use by the controllers. Instead of histograms, this display provides only the delay data, color-coded to indicate delay (dark green) or time advance (brownish green). Moreover, an arrowhead adjacent to the display indicates the trend in the evolving delay. For instance, the arrowhead pointing up indicates that the delay is increasing, while the arrowhead pointing in the downward direction indicates decreasing delay or improving time advance.

Downloaded by UNIVERSITY OF CALIFORNIA - BERKELEY on June 25, 2014 | http://arc.aiaa.org | DOI: 10.2514/6.2013-4236

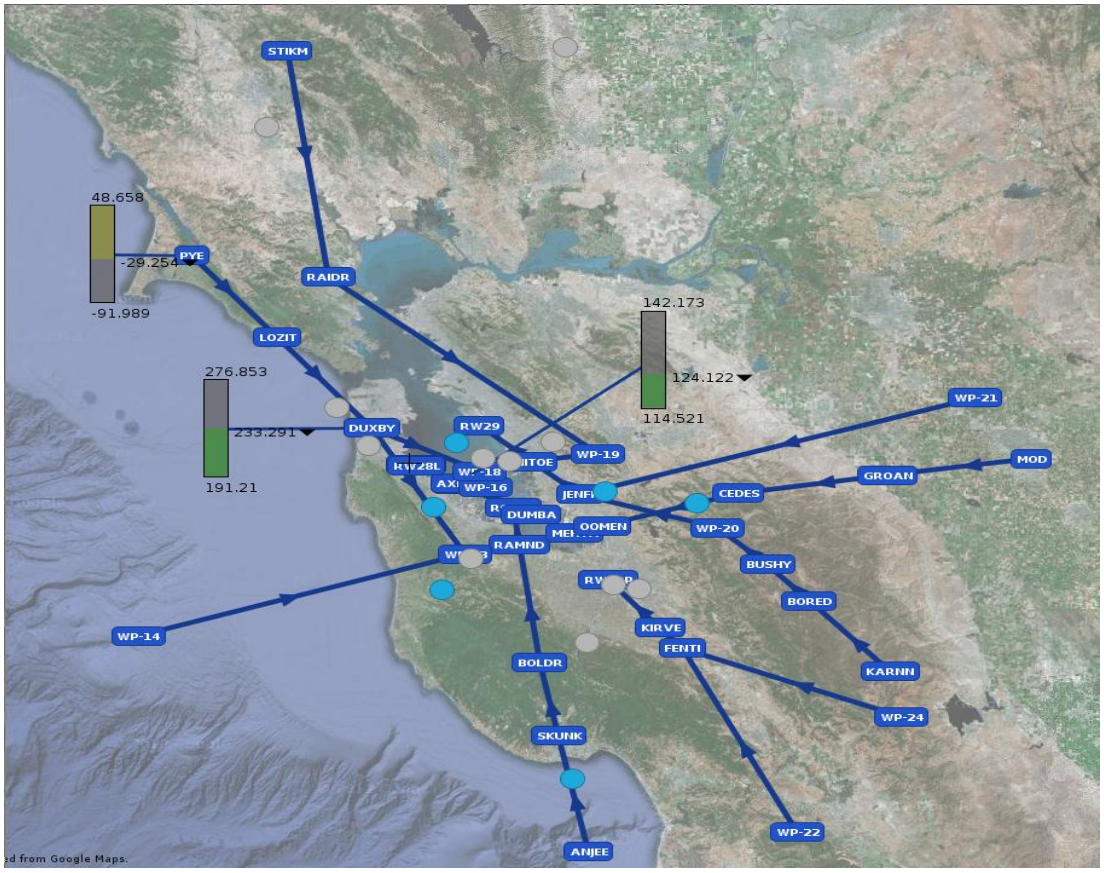

Figure 20. Display for Time Delay and its Time Rate for Branches

Air traffic controllers can use these delay displays to regulate the inflow into the terminal area, as well as to assess the regions of airspace encountering congestion. For example as shown in Figure 20, the route from PYE to KSFO Runway 28R, the later segments of DUXBY-AXMUL and AXMUL-RW28R exhibit delays, while the initial route segment of PYE-DUXBY does not encounter any delay in Figure 20.

V. Conclusions

The paper presented a methodology for estimating the traffic flow parameters from radar track data in the Terminal Area. The approach used a queuing network to capture the traffic flow characteristics using a few statistical parameters. The queuing network was constructed from published terminal area routes such as STARs, DPs and SIAPs. The routes were discretized into smaller servers to enforce separation requirements. Queuing parameters were estimated using a particle filter. Since the parameters in the queuing network have non-Gaussian distributions, and time-propagation models and measurement models were nonlinear, conventional estimation methods that resort to Gaussian and linearity assumptions were not applicable. By using the airspeed reports from radar track, it is shown that time-delay and its rate, together with the service time distribution, can be estimated. A graphical display for providing the time-delay monitoring to serve as a decision support tool to human controllers was also presented. The estimated queuing parameters can also be used to formulate decision support systems for triggering traffic flow management initiatives.

Acknowledgments

This research was supported under NASA Contract No. NX11CB70C, with Mr. Gary Lohr of NASA Langley Research Center serving as the Technical Monitor. Dr. Kara Latorella was the COR for this effort. The radar track data used in the research was from the FAA Automated Radar Terminal System at the San Francisco terminal area, and was provided to Optimal Synthesis, Inc. (OSI) by Mr. Michael C. McCarron, Director of Community Affairs and Mr. Bert Ganoung, Manager of the Aircraft Noise Abatement Office at the San Francisco International Airport. The queuing network model was generated using the Q-Gen software developed at OSI by Mr. Jason Kwan, under the

Downloaded by UNIVERSITY OF CALIFORNIA - BERKELEY on June 25, 2014 | http://arc.aiaa.org | DOI: 10.2514/6.2013-4236

direction of Dr. Monish Tandale. Thanks are due to Dr. Prasenjit Sengupta of OSI for several discussions on particle filter development.

References

[1]Grabbe, S. R., and Sridhar, B., "Integrated Traffic Flow Management Decision Making," *AIAA Guidance, Navigation, and Control Conference*, Chicago, IL, Paper AIAA-2009-6008, Aug. 10-13, 2009.

[2]Sun, D., Sridhar, B., and Grabbe. S. R., "Traffic Flow Management Using Aggregate Flow Models and the Development of Disaggregation Methods," *AIAA Guidance, Navigation, and Control Conference*, Chicago, IL, Paper AIAA-2009-6007, Aug. 10-13, 2009.

[3]Grabbe, S. R., Sridhar, B., and Mukherjee. A., "Sequential Traffic Flow Optimization with Tactical Flight Control Heuristics," *Journal of Guidance, Control, and Dynamics*, Vol.32, No.3, pp 810-820, May-Jun. 2009.

[4]Grabbe, S. R., and Sridhar, B., "Congestion Management with an Aggregate Flow Model," *AIAA Guidance, Navigation, and Control Conference and Exhibit*, San Francisco, CA, Paper AIAA-2005-6277, Aug. 15-18, 2005.

[5] Rios, J., and Lohn, J., "A Comparison of Optimization Approaches for Nationwide Traffic Flow Management," *AIAA Guidance, Navigation, and Control Conference*, Chicago, IL, Paper AIAA-2009-6010, Aug. 10-13, 2009.

[6]Rios, J., and Ross, K., "Massively Parallel Dantzig-Wolfe Decomposition Applied to Traffic Flow Scheduling," *AIAA Guidance, Navigation, and Control Conference*, Chicago, IL, Paper AIAA-2009-6009, Aug. 10-13, 2009.

[7]Rios, J., and Ross, K., "Parallelization of the Traffic Flow Management Problem," *AIAA Guidance, Navigation and Control Conference and Exhibit*, Honolulu, HI, Paper AIAA-2008-6519, Aug. 18-21, 2008.

[8]Rios, J., and Ross, K., "Solving High Fidelity, Large-Scale Traffic Flow Management Problems in Reduced Time," *8th AIAA ATIO Conference*, Anchorage, AK, Paper AIAA 2008-8910, Sep. 14-19, 2008.

[9]Berger, J. O., *Statistical Decision Theory and Bayesian Analysis*, Springer-Verlag, New York, NY, 1985.

[10]Cassandras, C. G., and Lafortune, S., *Introduction to Discrete Event Systems*, Kluwer Academic Publishers, Boston, MA, 1999.

[11]Saaty, T. L., *Elements of Queuing Theory with Applications*, Dover Publications, New York, NY, 1983.

[12]Bertsimas, D., "An Exact FCFS Waiting Time Analysis for a General Class of G/G/s Queuing Systems," *Queuing Systems*, Vol. 3, No. 4, December 1988, pp. 305–320.

[13]Bertsimas, D., "An Analytic Approach to a General Class of G/G/s Queuing Systems," *Operations Research*, Vol. 38, No. 1, Jan.-Feb. 1990, pp. 139–155.

[14]Menon, P. K., Tandale, M. D., Kim, J., Sengupta, P., Kwan, J. S., Palaniappan, K., Cheng, V. H. L., Subbarao, K., Rosenberger, J., "Multi-Resolution Queuing Models for Analyzing the Impact of Trajectory Uncertainty and Precision on NGATS Flow Efficiency," Report No. OSS-0704-01 submitted under NASA Contract No. NNA07BC55C, November 2008.

[15]Tandale, M. D., Menon, P. K., Cheng, V. H. L., Rosenberger, J., and Thipphavong, J., "Queueing Network Models of the National Airspace System," *8th AIAA Aviation Technology, Integration, and Operations (ATIO) Conference*, Anchorage, AK, Paper AIAA-2008-8942, Sep. 14-19, 2008.

[16] Kim, J., Palaniappan, K., Menon, P. K., Subbarao, K., and Thipphavong, J., "Trajectory Uncertainty Modeling for Queueing Analysis of the National Airspace System," *8th AIAA Aviation Technology, Integration, and Operations (ATIO) Conference*, Anchorage, AK, Paper 2008-8854, Sep. 14-19, 2008.

[17]Menon, P. K., Tandale, M. D., Kim, J., Sengupta, P., Kwan, J. S., Palaniappan, K., Cheng, V. H. L., Subbarao, K., Rosenberger, J., "Efforts to Validate Multi-Resolution Queuing Models," Report No. OSS-0704-02 submitted under NASA Contract No. NNA07BC55C, Optimal Synthesis Inc., Los Altos, CA, July 2009.

[18] Menon, P. K., Tandale, M. D., Kim, J., Sengupta, P., "A Framework for Stochastic Air Traffic Flow Modeling and Analysis," *2010 AIAA Guidance, Navigation and Control Conference*, Toronto, Canada, Aug. 2-5, 2010.

[19]Callantine T. J., "An Integrated Tool for NextGen Concept Design, Fast-Time Simulation and Analysis," *AIAA Modeling and Simulation Technologies Conference*, Honolulu, HI, Aug 18-21 2008.

[20]Callantine T. J., "TRAC Trial Planning and Scenario Generation to Support Super Density Operation Studies," *AIAA Modeling and Simulation Technologies Conference*, Chicago, IL, Aug 10 -13 2009.

[21]Gariel, M., Clarke, J.-P., and Feron, E, "A Dynamics I/O Model for TRACON Traffic Management," *Proceedings of the AIAA Guidance, Navigation, and Control Conference*, Hilton Head, SC, Aug 2007.

[22]Tandale, M.D., Vaddi, S., Wiraatmadja, S., and Cheng, V.H.L., "A Queuing Framework for Terminal Area Operations," *Proceedings of the AIAA Guidance, Navigation, and Control Conference*, Portland, OR, Aug 2011.

[23]Sengupta, P., Tandale, M.D., Cheng, V.H.L., and Menon, P.K., "Air Traffic Estimation and Decision Support for Stochastic Flow Management," *Proceedings of the AIAA Guidance, Navigation, and Control Conference*, Portland, OR, Aug 2011.

[24]Thrun, S., Burgard, W. and Fox, D., *Probabilistic Robotics*, The MIT Press, Cambridge, MA, 2005.

[25]Gelb, A. (Editor), *Applied Optimal Estimation*, MIT Press, Cambridge, MA, 1989.

[26]Ristic, B., Arulampalam, S., and Gordon, N., *Beyond Kalman Filter*, Artech House, Boston, MA, 2004.

[27]Arulampalam, M. S., Maskell, S., Gordon, N. and Clapp, T., "A Tutorial on Particle Filters for Online Nonlinear/Non-Gaussian Bayesian Tracking," *IEEE Transactions on Signal Processing*, Vol. 50, No. 2, pp. 174-188, 2002.

Downloaded by UNIVERSITY OF CALIFORNIA - BERKELEY on June 25, 2014 | http://arc.aiaa.org | DOI: 10.2514/6.2013-4236

[28]Hol, J.D., Schon,T.B., and Gustafsson, F., "On Resampling Algorithms for Particle Filters," Proceedings of IEEE Nonlinear Statistical Signal Processing workshop, pp.79-82, 2006.
[29]SFO WestPlan and South-East Plan Configurations: http://www.flysfo.com/web/page/about/news/pressres/ [cited 16 July 2013]
[30]Federal Aviation Administration: Coded Instrument Flight Procedures (CIFP): http://www.faa.gov/air_traffic/flight_info/aeronav/productcatalog/digitalproducts/nfd/ [cited 16 July 2013]

Downloaded by UNIVERSITY OF CALIFORNIA - BERKELEY on June 25, 2014 | http://arc.aiaa.org | DOI: 10.2514/6.2013-4236